Photonic Frequency Translation with EML+TIA Enabled Down-Converting Receiver

Aina Val Martí[(1)], Nemanja Vokić[(1)], Dinka Milovančev[(1)], Thomas Zemen[(1)], Fotini Karinou[(2)], and Bernhard Schrenk[(1)]

[(1)]AIT Austrian Institute of Technology, 1210 Vienna, Austria. Author e-mail: aina.val-marti@ait.ac.at
[(2)] Microsoft Research Ltd., Cambridge CB1 2FB, United Kingdom.

Abstract *We experimentally demonstrate the transparent conversion of an OFDM signal in the K_a-band (35GHz) to a sub-6GHz frequency, using an EML+TIA coherent receiver. We further prove sideband-suppressed reception for this simplified receiver through confirming dispersion-tolerant mm-wave transmission, in contrast to direct-detection with RF down-conversion.*

Introduction

With the increase in signal bandwidth and the exploration of higher signal frequencies in mm-wave bands and beyond, transparent frequency translation from a low to a high carrier frequency, and vice versa, becomes a necessity. Porting such a tool to the optical domain can be highly beneficial for applications such as optically fronthauled radio access, photonics-augmented RF-ADCs [1] or frequency conversions blocks for satellite comms [2]. While frequency up-conversion techniques are rather well researched and have been demonstrated by means of optical carrier suppression [3, 4], independent sideband modulation [5], comb sources with selective modulation of their spectral lines [6, 7] and heterodyning with free-running lasers [8], down-conversion techniques enjoy considerably less attention. Although earlier works have demonstrated the concept to be feasible [1, 2, 9], its complexity is typically exceeding that of up-conversion techniques.

In this work, we propose and experimentally demonstrate a simplified approach for photonic down-conversion of mm-wave signals relying on frequency-synchronous coherent detection. We show that an electro-absorption modulated laser (EML) integrated with a transimpedance amplifier (TIA) can cater for the needs of translating an OFDM signal from 35.1 to 3.5 GHz. Comparison with a direct-detection receiver and RF-based down-conversion further reveals that dispersion-induced fading effects can be effectively mitigated by virtue of the sideband-suppression property of the proposed EML+TIA receiver.

EML as a *f*-Downconverting Receiver

The proposed down-conversion process in this work is contributed by the frequency-selective reception of a coherent EML+TIA receiver. The frequency- and phase synchronous detection with an EML-based homodyne receiver has been introduced earlier [10]: Through injection-locking of its distributed feedback (DFB) laser section, we obtain a local oscillator (LO) that is adjusted to a specific spectral line of the optical input signal to the EML. Its electro-absorption modulator (EAM) section then serves as the photodiode where LO and input signal beat. Although this concept has been thoroughly proven in the past, the possibility of photonic down-conversion has not been investigated up to now: The spectral line can be any feature of the optical signal, such as the optical carrier Λ of a dual-sideband signal, as introduced in Fig. 1, or a virtual carrier (VC) appended to a data signal – provided that it is sufficiently strong to enable a locking range (LR) within which the EML emission Λ_{EML} locks to the input signal. In case that the EML is locked to a VC, the adjacent data signal (u) is down-converted to the baseband, while its optical carrier Λ and the second sideband (l) can be suppressed through simple lowpass filtering or bandwidth limiting.

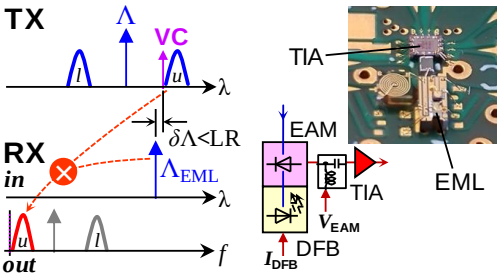

Fig. 1: Photonic frequency translation with EML+TIA.

The coherent EML+TIA receiver builds on a chip-on-carrier O-band EML co-integrated with a die-level TIA (Fig. 1). The EML at 1299 nm yields a fiber-coupled power of 6 dBm at 100 mA. The LR is 1 GHz for an input of -24.5 dBm. The DC component of the EAM photocurrent is dropped before the TIA with an RF bias-T. The opto-electronic 3dB bandwidth of the EML+TIA assembly is 6.1 GHz. Details are reported in [11].

Down-Conversion of mm-Wave Signals

We evaluated the photonic down-conversion functionality of the EML+TIA receiver for frequency translation from the mm-wave to the baseband (Fig. 2). An arbitrary waveform generator (AWG) provides an OFDM data signal

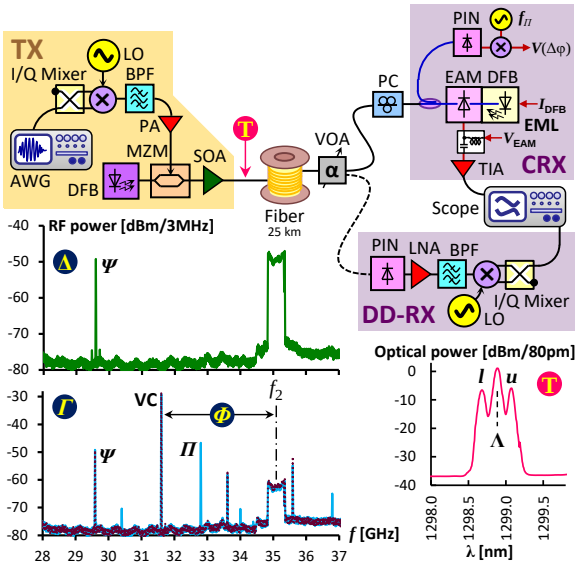

Fig. 2: Setup and transmitted RF / optical spectra.

at 5.5 GHz with 128 subcarriers over a bandwidth of 500 MHz, together with an additional 3.5 GHz pilot tone. Both are up-converted to a mm-wave RF carrier at 29.6 GHz. The signal is modulated as double sideband signal on an optical carrier at 1298.9 nm (inset T in Fig. 2) using a simple Mach-Zehnder modulator (MZM).

Figure 2 also presents the transmitted mm-wave signals without (Δ) and with (Γ) pilot tone, which is taking the role as a VC for the photonic down-conversion process at the receiver. The OFDM signal at the RF carrier at f_2 = 35.1 GHz is accompanied by the residual RF-LO note Ψ, resulting from the finite suppression of the up-conversion LO. The VC is spaced by Φ = 3.5 GHz from the OFDM center frequency. This defines the later intermediate frequency (IF) to which the OFDM signal will be down-converted. The VC power has been chosen to be ~10 dB stronger than the aggregated OFDM power. This is motivated by the need for stable locking at reasonable received optical power (ROP) levels at the EML+TIA receiver. Still, acceptable EVM performance will be found for the received OFDM signal, as will be proven shortly.

The optical mm-wave signal is then boosted by a semiconductor optical amplifier (SOA) and transmitted over a fiber span. A variable optical attenuator (VOA) sets the optical budget of the transmission link. We used two different receivers to compare the reception performance of the mm-wave signal: The coherent receiver (CRX) capitalizes on the EML+TIA to perform photonic down-conversion to the sub-6GHz range through locking on the VC. A polarization controller (PC) is needed due to the single-polarization architecture of the CRX, however, the polarization-independent operation of EML receivers has been proven earlier [12]. A direct-detection receiver (DD-RX) with a 40G PIN+TIA with subsequent RF down-conversion serves as the reference. EVM measurements have been conducted as function of the ROP to assess the reception performance.

Coherent Receiver Locking on Virtual Carrier

We locked the EML+TIA receiver on the VC component of the optical mm-wave signal to accomplish opto-electronic frequency translation of the OFDM signal from f_2 to Ψ. Although we have characterized the locking range of the EML to be ~160 MHz for the set ROP of -30 dBm, we further investigated the stability of the CRX locking with a simple monitoring circuit. For this purpose, an additional pilot Π has been included at an offset of 1.2 GHz from the VC (Fig. 2). While the VC falls at f = 0 upon locking, the pilot Π resides. Moreover, the pilot Π is partially reflected at the EML front-facet and detected together with the optical LO of the EML at a PIN receiver, whose beat note at f_B = 1.2 GHz is then phase discriminated with an auxiliary RF-LO at $f_\Pi = f_B$. With this, the optical phase of the EML emission, which is determined by the relative mismatch between the free-running EML and input signal wavelengths [13], can be directly acquired and used to tune its DFB-LO through adjusting the DFB bias current [14]. However, as the spectrogram in Fig. 3a proves, stable locking is accomplished even without closed-loop DFB control: Upon locking the DFB-LO to the input signal at time instance τ, we observe a stable OFDM signal reception at the IF of Φ = 3.5 GHz. The detected phase of the pilot Π swings with an acceptable peak-to-peak deviation of ς = 52°, which is attributed to slow effects concerning the temperature control of the

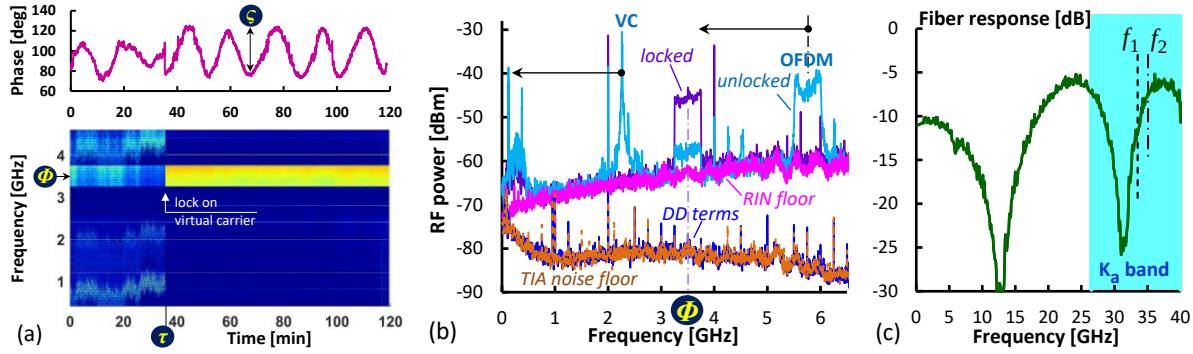

Fig. 3: (a) Locking stability of the CRX and (b) signal spectra received by the EML+TIA. (c) NZ-DSF response at 1299 nm.

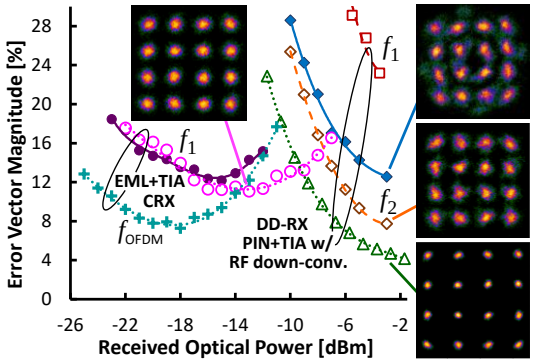

Fig. 4: Reception performance for DD-RX with RF-based down-conversion and CRX with photonic down-conversion.

EML ($\delta\nu_{EML}/\delta T$ = 11.8 GHz/K). Under these conditions, we found no excursions that indicate the loss of locking over more than one hour.

Reception Performance under f-Translation

Figure 3b shows the received signal spectra after photonic down-conversion with the CRX for typical input power of -15 dBm. When the CRX is not locked, the VC and OFDM signal are both visible (before tuning the VC to 0 Hz to lock the EML). Under locking, the OFDM is received at the desired IF of Φ = 3.5 GHz. It proves the VC-assisted down-converion principle to be feasible. The SNR of the OFDM is then limited by the relative intensity noise (RIN) floor of the EML emission. A balanced EML detector could suppress this RIN noise and eventually recover the SNR offset of ~15 dB at Φ towards the TIA noise floor. When leaving the DFB section of the EML unbiased, yet an optical signal is present at the input of the CRX, the received signal spectrum still overlaps with that of the TIA noise. This confirms that direct-detection terms are not impacting the signal reception, which can be expected to some degree since the mm-wave signal is out of the sub-6GHz reception band.

To further investigate the reception performance for both detection methodologies with respect to dispersion-induced signal fading, which is recognized as a critical impairment for double-sideband modulated high-frequency signals, we employed an ITU-T G.655 fiber in the transmission link. This is because the EML that furnishes the CRX is operating around 1299 nm, where ITU-T G.652 SSMF fiber has minimal dispersion. Therefore, to make the results transferrable to C-band applications, we instead used non-zero dispersion shifted fiber (NZ-DSF) with a dispersion of -8 ps/(nm·km). The e/o/e response of a 25-km long fiber span is characterized in Fig. 3c. As can be well noticed, there is a wide spectral notch covering more than half of the K_a-band region of the mm-wave spectrum. We therefore investigated two cases, where the OFDM signal is transmitted at two different mm-wave carrier frequencies f_1 and f_2 at the slope of the dispersion-induced notch.

Figure 4 reports the EVM performance for the CRX based on EML+TIA and the DD-RX building on PIN+TIA and RF down-converter.

For the **DD-RX** in back-to-back configuration without fiber (△), we obtain a low EVM of 4.2% at a ROP of -1.7 dBm. With a transmission fiber we see an EVM increase of 3.5% for the mm-wave carrier at f_2 (◇). We attribute this penalty to the dispersion-induced fading. The RF-based down-conversion additionally requires frequency synchronization between the synthesizers at the mm-wave transmitter and receiver. If the down-conversion RF-LO is not synchronized to the respective LO at the transmitter, we see an additional EVM penalty of 4.9% (◆). Moreover, the EVM sharply increases to >20% (□) at the alternative carrier frequency f_1, which is severely impacted by dispersion-induced fading (Fig. 3c). This renders transmission unfeasible.

For the **CRX**, the back-to-back sensitivity (○) improves by ~13 dB with respect to the DD-RX. The accomplishable EVM minimum of 11.1% is higher due to the RIN noise and the residual non-linearity of the receiver, as discussed in [11]. Still, it is below the 12.5% EVM limit for 16-QAM OFDM transmission. At the worse mm-wave carrier frequency f_1, there is now no penalty in presence of the NZ-DSF span (●). This penalty, clearly visible for the DD-RX, has been fully recovered through suppression of the second modulation sideband by locking on the CRX on the VC, thus mitigating dispersion-induced fading. As a second beneficial aspect of the photonic down-conversion with the EML+TIA, the RF plane of the receiver is simplified due to the omission of RF mixer and synchronized mm-wave LO. Finally, we have included the case where the CRX is locked on the optical carrier Λ while the OFDM signal is transmitted in the baseband at f_{OFDM} = 3.5 GHz (+). Here, we accomplish an EVM of 7.3% at a ROP of -18 dBm. The improvement is attributed to the better dynamic DAC range of the AWG for an OFDM signal without strong VC.

Conclusions

We have demonstrated the substitution of RF-based down-conversion through a selectively locked coherent receiver based on a simplified EML+TIA architecture. We accomplished signal reception for 16-QAM OFDM below the EVM antenna limit while translating the OFDM carrier frequency from 35.1 to 3.5 GHz. Dispersion-tolerant mm-radio transmission is enabled by virtue of the sideband selectivity of the CRX.

Acknowledgements

This work was supported by the ERC under the EU Horizon-2020 programme (grant nº 804769) and by the Austrian FFG agency through the PHIDELITI project (grant n° 883894).

References

[1] N. P. O'Malley, K. A. McKinzie, M. S. Alshaykh, J. Liu, D. E. Leaird, T. J. Kippenberg, J. D. McKinney, and A. M. Weiner, "Architecture for integrated RF photonic downconversion of electronic signals," *Optics Letters*, vol. 48, no. 1, pp. 159-162, 2023. DOI: 10.1364/OL.474710

[2] S. Zhu, X. Fan, M. Li, N. H. Zhu, and W. Li, "Microwave photonic frequency down-conversion and channel switching for satellite communication," *Optics Letters*, vol. 45, no. 18, pp. 5000-5003, 2020. DOI: 10.1364/OL.398495

[3] S. Yu, W. Gu, A. Yang, T. Jiang and C. Wang, "A Frequency Quadrupling Optical mm-Wave Generation for Hybrid Fiber-Wireless Systems," *IEEE Journal on Selected Areas in Communications*, vol. 31, no. 12, pp. 797-803, 2013. DOI: 10.1109/JSAC.2013.SUP2.12130012.

[4] Z. Xu, X. Zhang, and J. Yu, "Frequency upconversion of multiple RF signals using optical carrier suppression for radio over fiber downlinks," *Optics Express*, vol. 15, no. 25, pp. 16737-16747, 2007. DOI: 10.1364/OE.15.016737

[5] A. Val-Martí, N. Vokić, T. Zemen and B. Schrenk, "Hybrid CAP / mm-wave OFDM Vector Modulation for Photonic Frequency Conversion in a Single-Sideband Feeder," *2022 Optical Fiber Communications Conference and Exhibition (OFC)*, San Diego, USA, Mar. 2022, Th1I.3. DOI: 10.1364/OFC.2022.Th1I.3

[6] K. Zeb, Z. Lu, J. Liu, Y. Mao, G. Liu, P.J. Poole, M. Rahim, G. Pakulski, P. Barrios, M. Vachon, D. Poitras, W. Jiang, J. Weber, X. Zhang, and J. Yao, "Broadband Optical Heterodyne Millimeter-Wave-over-Fiber Wireless Links Based on a Quantum Dash Dual-Wavelength DFB Laser," *Journal of Lightwave Technology*, vol. 40, no. 12, pp. 3698-3708, 2022. DOI: 10.1364/JLT.40.003698

[7] K. Li and J. Yu, "Photonics-Aided Terahertz-Wave Wireless Communication," in *Journal of Lightwave Technology*, vol. 40, no. 13, pp. 4186-4195, 2022. DOI: 10.1109/JLT.2022.3161878.

[8] J. Zhang, M. Zhu, M. Lei, B. Hua, Y. Cai, Y. Zou, L. Tian, A. Li, Y. Wang, Y. Huang, J. Yu, and X. You, "Real-time demonstration of 103.125-Gbps fiber–THz–fiber 2 × 2 MIMO transparent transmission at 360–430 GHz based on photonics," *Optics Letters*, vol. 47, no. 5, pp. 1214-1217, 2022. DOI: 10.1364/OL.448064

[9] D. Wang, F. Yang, Y. Wang, Z. Chen, D. Yang and F. Wu, "Filter-Free Photonic Image-Rejection Down-Conversion for Distributed Antenna Applications," *IEEE Photonics Journal*, vol. 13, no. 2, pp. 1-10, 2021. DOI: 10.1109/JPHOT.2021.3064553.

[10] B. Schrenk, "The Electroabsorption-Modulated Laser as Optical Transmitter and Receiver: Status and Opportunities," *IET Optoelectronics*, vol 14, no. 10, pp. 1049, 2020. DOI: 10.1049/iet-opt.2020.0010

[11] D. Milovančev, N. Vokić, F. Karinou and B. Schrenk, "Simplified Coherent Receiver for Analogue Radio Transmission Over High Optical Budgets," *Journal of Lightwave Technology*, vol. 39, no. 24, pp. 7672-7681, 2021. DOI: 10.1109/JLT.2021.3085517

[12] B. Schrenk, and F.Karinou, "Simple Laser Transmitter Pair as Polarization-Independent Coherent Homodyne Detector," *Optics Express*, vol. 27, no. 19, pp. 13942-13950, 2019. DOI: 10.1364/OE.27.013942

[13] F. Mogensen, H. Olesen, and G. Jacobsen, "Locking Conditions and Stability Properties for Semiconductor Laser with External Light Injection," *IEEE Journal of Quantum Electronics*, vol. 21, no. 7, pp. 784-793, Jul. 1985. DOI: 10.1109/JQE.1985.1072760

[14] Z. Liu, and R. Slavík, "Optical Injection Locking: From Principle to Applications," *Journal of Lightwave Technology*, vol. 38, no. 1, pp. 43-59, 2020. DOI: 10.1109/JLT.2019.2945718